Brainstem angiocentric gliomas with MYB-QKI rearrangements

Laura D'Aronco[1,*], **Cécile Rouleau**[3,*], **Tenzin Gayden**[3], **Louis Crevier**[4], **Jean-Claude Décarie**[5], **Sébastien Perreault**[6], **Nada Jabado**[3], **Pratiti Bandopadhayay**[3], **Keith L. Ligon**[7], and **Benjamin Ellezam**[1]

[1]Departments of Pathology, Sainte-Justine Hospital, Université de Montréal, Montréal, Québec, Canada.

[2]Department of Pediatrics, McGill University and McGill University Heath Centre Research Institute, Montréal, Québec, Canada.

[3]Departments of Pediatric Oncology, Dana-Farber Cancer Institute, Boston Children's Hospital, Boston, Massachusetts, USA

[4]Department of Surgery, Sainte-Justine Hospital, Université de Montréal, Montréal, Québec, Canada.

[5]Department of Radiology, Sainte-Justine Hospital, Université de Montréal, Montréal, Québec, Canada.

[6]Department of Pediatrics, Sainte-Justine Hospital, Université de Montréal, Montréal, Québec, Canada.

[7]Departments of Pathology,Dana-Farber Cancer Institute, Boston Children's Hospital, Boston, Massachusetts, USA

Keywords

Angiocentric glioma is a low-grade CNS tumor typically found in the cerebral hemispheres where it causes refractory epilepsy [4]. Surgical resection is often sufficient for seizure control and the rate of tumor recurrence is low [1]. On pathology, this neoplasm shares some cytologic features with pilocytic astrocytoma but is differentiated by its specific vascular polarity, its infiltrative growth pattern, and its epithelial membrane antigen (EMA) immunoreactivity [4]. In an initial study, a MYB-QKI rearrangement was present in 6 of 7 angiocentric gliomas and absent in 147 other gliomas, making it a potential diagnostic marker in ambiguous or atypical cases [2]. A subsequent study of a large number of cerebral low grade gliomas confirmed the specificity of MYB-QKI rearrangements for angiocentric gliomas [5]. A midbrain tumor resembling angiocentric glioma was previously reported but presence of the rearrangement was not assessed [3]. Here, we report two cases of brainstem angiocentric gliomas with evidence of MYB-QKI rearrangements.

Corresponding author: Benjamin Ellezam, Benjamin.ellezam@umontreal.ca, Phone: 1-514-825-6667, Fax: 1-514-345-4819.
*These authors contributed equally to the work

Case 1

A 7-year-old boy, known for late verbal and motor milestones, and treated for chronic cough and recurrent pneumonia, had recently consulted for progressive respiratory failure. Investigations suggested the presence of micro-aspirations and revealed a swallowing disorder, sialorrhea and obstructive sleep apnea. A slight gait instability was also noted, raising the possibility of a CNS etiology. Brain MRI revealed a non-enhancing, T1-hypointense T2/FLAIR-hyperintense mass, expanding the pons and the medulla, with diffuse infiltration along the right cerebellar peduncle and exophytic growth partially compressing the 4th ventricle, without hydrocephalus (Figure 1E–G). Stereotactic needle biopsy of the exophytic component was performed.

Cytologic smear showed monomorphic cells with long fibrillary processes and elongated nuclei abutting blood vessels, aligned with their longitudinal axis (Figure 1B). The chromatin was finely speckled, without atypia. The histology was generally hypocellular and inconspicuous glial tumor cells growing along blood vessels mimicked microvascular proliferation (Figure 1A–C). The growth pattern was diffusely infiltrative, with several entrapped neurons (Figure 2A) and neurofilament-immunopositive underlying axons (not shown). Tumor cells sometimes showed perpendicular alignment of fibrillar processes around blood vessels (Figure 2A *inset*). Despite the low density and fibrillary morphology reminiscent of pilocytic astrocytoma, the angiocentricity was deemed atypical for this entity. No Rosenthal fibers or eosinophilic granular bodies were present. Staining for EMA (clone E29, Dako) revealed both surface and cytoplasmic microlumen-type immunoreactivity in a pattern characteristic of angiocentric glioma (Figure 2D). Staining for EMA on 12 archival pilocytic astrocytomas was entirely negative (not shown). The Ki-67 proliferation index was 0%. There was no mitotic activity, necrosis, or microvascular proliferation. Immunohistochemistry for P53, IDH1 R132H, H3 K27M and ATRX showed wild-type patterns. Immunohistochemistry for MYB showed expression in tumor cells (not shown). Further molecular characterization by FISH and by PCR-based high resolution melting point analysis (HRM) excluded the KIAA1549-BRAF fusion and BRAF V600E mutation, respectively. Whole transcriptome sequencing performed on fresh frozen tissue revealed a MYB-QKI rearrangement involving exon 15 of MYB (chr6:135,524,462) and exon 5 of QKI (chr6:163,983,014) and the fusion transcript was validated using RT-PCR followed by Sanger sequencing (Figure 2H).

Given the unresectable nature of the tumor, the patient was treated with chemotherapy including carboplatin and vincristine. After four months of treatment, the patient showed signs of clinical progression with a new right sixth nerve palsy and difficulty initiating horizontal saccades. Control MRI was however stable. The patient was started on weekly vinblastine and bevacizumab was added six months later when patient showed clinical progression with a new mild left side paresis. MRI continued to show stable tumor size despite clinical deterioration.

Case 2

A 3-year-old boy who presented with right seventh nerve palsy showed a brainstem tumor with essentially the same MRI characteristics (Figure 2E–G) and histology (Figure 2A–D) as case 1. Targeted next generation DNA sequencing (OncoPanel™) showed chromosome 6q loss with intragenic breaks in MYB and QKI suggesting a fusion/rearrangement event (Figure 2H).

The patient was treated with carboplatin and vincristine for one year. He was initially stable but showed increased symptoms and signs three years later and was treated with bevasizumab for two months. Tumor progression was noted and therapy switched to m-TOR inhibitor everolimus with initial response in tumor size. Patient has now been stable for 10 months with ongoing treatment.

To our knowledge, these are the first reported cases of brainstem angiocentric glioma with the characteristic MYB-QKI rearrangement. It highlights the importance of molecular analysis and fresh frozen tissue procurement in resolving diagnosis, particularly in small-size stereotactic biopsies. In contrast to previous reports of supratentorial angiocentric glioma, our patients presented slow but progressive clinical deterioration. Based on our observation, incompletely resected brainstem angiocentric glioma might not have a benign behavior and can lead to severe cranial neuropathies and brainstem dysfunction over years.

References

1. Ampie L, Choy W, DiDomenico JD, Lamano JB, Williams CK, Kesavabhotla K, Mao Q, Bloch O (2016) Clinical attributes and surgical outcomes of angiocentric gliomas. J Clin Neurosci 28: 117–122 Doi 10.1016/j.jocn.2015.11.015 [PubMed: 26778052]

2. Bandopadhayay P, Ramkissoon LA, Jain P et al. (2016) MYB-QKI rearrangements in angiocentric glioma drive tumorigenicity through a tripartite mechanism. Nat Genet 48: 273–282 Doi 10.1038/ng.3500 [PubMed: 26829751]

3. Covington DB, Rosenblum MK, Brathwaite CD, Sandberg DI (2009) Angiocentric glioma-like tumor of the midbrain. Pediatr Neurosurg 45: 429–433 Doi 10.1159/000277616 [PubMed: 20110754]

4. Burger PC, Jouvet A, Preusser M, Rosenblum MK, Ellison DW (2016) Angiocentric Glioma In: Louis DN, Ohgaki H, Wielster OD, Cavenee WK, Ellison DW, Figarella-Branger D, Perry A, Reifenberger G, Von Deimling A (eds) WHO Classification of Tumours of the Central Nervous System, revised 4th edn Internationnal Agency for Research on Cancer, Lyon, pp 119–120

5. Qaddoumi I, Orisme W, Wen J et al. (2016) Genetic alterations in uncommon low-grade neuroepithelial tumors: BRAF, FGFR1, and MYB mutations occur at high frequency and align with morphology. Acta Neuropathol. 131:833–45. doi: 10.1007/s00401-016-1539-z. [PubMed: 26810070]
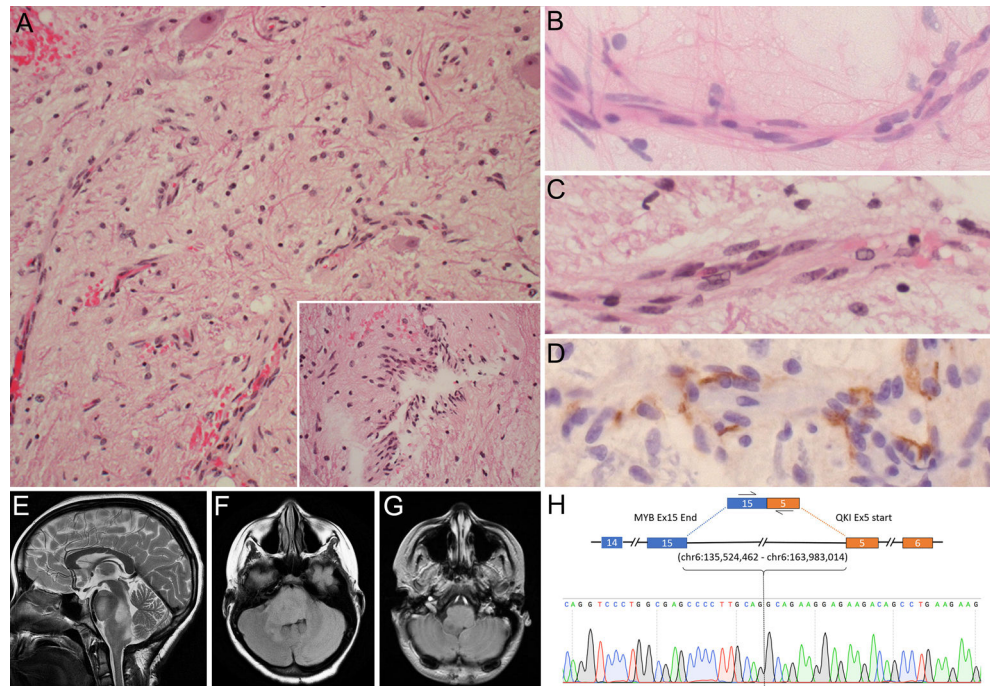
Fig. 1.

Case 1. Photomicrographs of representative H&E tissue section (**A**) showing low-cellularity glial tumor with growth along blood vessels or in a perpendicular orientation (**inset)**, with entrapped neurons. Cytologic smear (**B**) and tissue section (**C**) highlighting longitudinal growth along blood vessels and elongated nuclei with finely speckled chromatin. **D** Immunohistochemistry for EMA showing surface and cytoplasmic positivity. MRI images showing a T2-hyperintense (**E**), FLAIR-hyperintense (**F**), T1-hypointense non-contrast enhancing (**G**), dorsally exophytic mass infiltrating pons and medulla. (**H**) Sanger sequencing of MYB-QKI fusion transcript. Initial magnification in *A*, 200x; *inset*, 400x; *B-D, 630x*
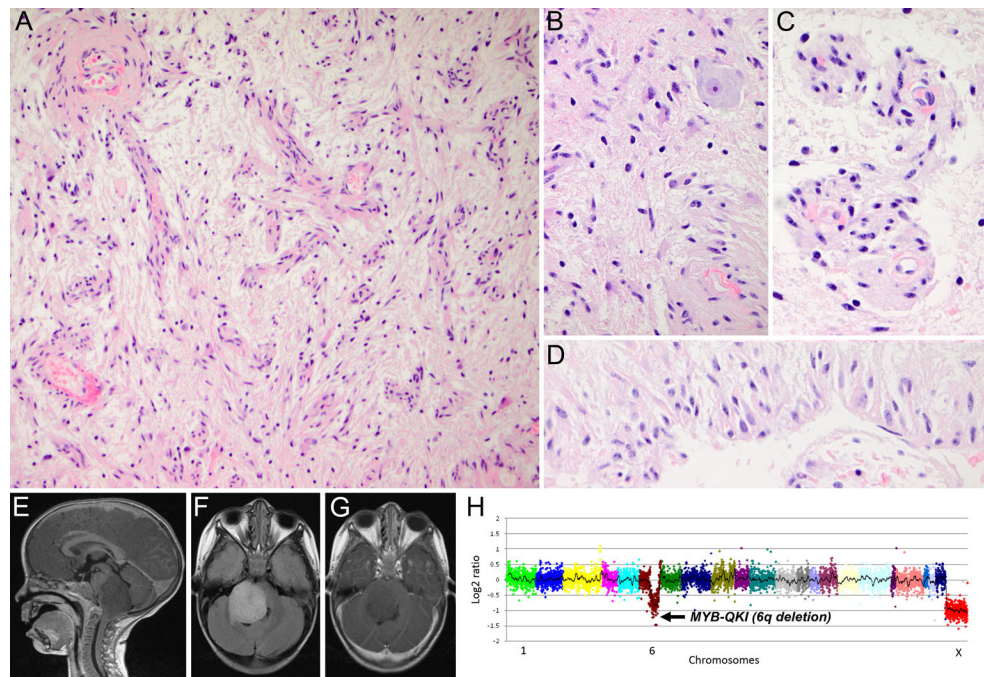
Fig. 2.
Case 2. Photomicrographs of representative H&E tissue sections showing low-cellularity glial tumor with angiocentric growth (**A** and **C**), entrapped neurons (**B**), and growth in a perpendicular orientation (**D**). MRI images showing a T1-hypointense (**E**), FLAIR-hyperintense (**F**), non-contrast enhancing (**G**), dorsally exophytic mass infiltrating pons and medulla. **H** Next-generation sequencing (OncoPanel^TM) showing 6q deletion suggestive of MYB-QKI fusion. Initial magnification in *A*, 200x; *B-D, 600x*